RasV12 Expression in Microglia Initiates Retinal Inflammation and Induces Photoreceptor Degeneration

Yuta Moriuchi,[1] Toshiro Iwagawa,[1] Asano Tsuhako,[1] Hideto Koso,[1] Yasuyuki Fujita,[2] and Sumiko Watanabe[1]

[1]Division of Molecular and Developmental Biology, Institute of Medical Science, University of Tokyo, Tokyo, Japan
[2]Department of Molecular Oncology, Graduate School of Medicine, Kyoto University, Kyoto, Japan

Correspondence: Sumiko Watanabe. Division of Molecular and Developmental Biology, Institute of Medical Science, University of Tokyo, 4-6-1 Shirokane-dai, Minato-ku, Tokyo 108-8639, Japan; sumiko@ims.u-tokyo.ac.jp.

Received: May 25, 2020
Accepted: November 5, 2020
Published: November 24, 2020

Citation: Moriuchi Y, Iwagawa T, Tsuhako A, Koso H, Fujita Y, Watanabe S. RasV12 expression in microglia initiates retinal inflammation and induces photoreceptor degeneration. *Invest Ophthalmol Vis Sci.* 2020;61(13):34. https://doi.org/10.1167/iovs.61.13.34

Purpose. The role of activated retinal microglia in driving retinal degeneration has been implicated in a number of in vivo disease models. Here, we investigated the primary consequences of microglial activation by the specific expression of constitutively active Ras in microglia in a transgenic mouse model before the onset of any degenerative changes in the retina.

Methods. The double transgenic lines *CAG-LSL-RasV12-IRES-EGFP; Cx3cr1*$^{CreER/+}$ (Cx3cr1-RasV12 mice) and *CAG-LSL-EGFP*; *Cx3cr1*$^{CreER_+}$ (control mice) were generated. The expression of RasV12 was induced in microglia by tamoxifen administration, and the retinas were examined by immunohistochemistry of frozen sections, RT-qPCR, and live imaging.

Results. RasV12 expression in retinal microglial cells promoted cell proliferation, cytokine expression, and phagocytosis. RasV12-expressing microglia migrated toward the inner and outer layers of the retina. Examination of glial fibrillary acidic protein (GFAP) expression revealed activation of Müller glia in the retina. We also observed loss of the photoreceptors in the outer nuclear layer in close proximity to microglial cells. However, no significant neurodegeneration was detected in the inner nuclear layer (INL) or ganglion cell layer (GCL). The morphology of RasV12-expressing microglia in the GCL and INL retained more ramified features compared with the predominantly-ameboid morphology found in outer retinal microglia.

Conclusions. The expression of RasV12 is sufficient to activate microglia and lead to photoreceptor degeneration. Neurons in the inner side of the retina were not damaged by the RasV12-activated microglia, suggesting that microenvironment cues may modulate the microglial phenotypic features and effects of microglial activation.

Keywords: microglia, retina, RasV12, transgenic mice, cytokines, phagocytosis

Microglia are tissue-resident macrophage-like cells, found throughout the central nervous system (CNS). Microglia play central roles in orchestrating immune responses in the CNS.[1] Recent evidence also suggests that microglia are involved in the pathogenesis of diseases associated with neuronal cell death through phagocytosis and secretion of inflammatory cytokines.[2] Therefore the development of strategies to modulate microglial activities has emerged as a promising approach to treat neurodegenerative diseases.

Microglia have also been implicated in several pathological conditions in the retina, including glaucoma and photoreceptor degeneration. Under physiological conditions, retinal microglia display ramified morphologies and are primarily found in the inner plexiform layer (IPL) and the outer plexiform layer (OPL). During development, retinal microglia promote neuronal cell survival by secreting neurotrophic factors and maintaining synaptic structures.[3] Retinal photoreceptor degeneration is accompanied with microglial activation. Upon activation, microglial cells undergo morphologic alterations, acquiring ameboid shapes. Activated microglial cells migrate to the site of degeneration, the outer nuclear layer (ONL), and subretinal regions (SR).[4,5] Several studies demonstrated the critical role of microglia in the onset and progression of retinal degeneration, by exerting neurotoxic effects on activation. In the rd10 mouse model, microglial activation promoted photoreceptor apoptosis in an IL-1β-dependent manner, aggravating retinal degeneration.[6] Consistently, administration of minocycline ameliorated retinal degeneration in the rd10 mouse model.[7] However, the elucidation of the role of microglia in photoreceptor degeneration remains challenging because of the complexity of the retinal structure and immunological circuits involved in retinal diseases. Rod photoreceptors secrete alarmins, such as Endothelin 2 (Edn2).[8] Alarmins and other cytokines activate Müller glial cells (MGCs), which upon activation, secrete various cytokines, including leukemia inhibitory factor (LIF).[9,10] Furthermore, the retinal pigment epithelium is often involved in immune responses under pathologic

Copyright 2020 The Authors

This work is licensed under a Creative Commons Attribution-NonCommercial-NoDerivatives 4.0 International License.

Downloaded from intl.iovs.org on 04/26/2024

conditions,[11] further increasing the complexity of the mechanisms underlying retinal inflammation.

Ras is a central signal transducer, functioning as a GDP/GTP-regulated molecular switch (GTPase). Ras activation triggers several downstream signaling pathways, including the RAF/MEK/ERK cascade. The Ras superfamily consists of various related proteins; H-Ras, N-Ras, and K-Ras4A/B are the most common Ras proteins in mammals.[12] K-Ras is activated by various transmembrane receptors that induce microglial activation, including CSF1 receptor (CSF1R), Fc gamma receptor (FcγR), and TREM2.[13–15] Aberrant Ras activation promotes oncogenesis, and Ras mutations have been identified in a wide variety of human cancers.[12] Mutation in V12 position of the Ras had been most frequently observed in cancer,[16] and substitution of G12 with V in H-Ras (H-RasV12) results in a constitutively active form. The mutant had been examined in many previous studies for molecular analyses of receptor activation and aberrant cell growth. A previous work using mouse BV-2 microglial cell line showed that inhibition of Ras farnesyl protein transferase suppressed the expression of iNOS.[17] Furthermore, the expression of RasV12 was sufficient to activate the expression of iNOS and NF-κB signaling pathway, which plays pivotal roles for induction of inflammatory cytokines, in mouse BV-2 microglial cell line.[17] The serine/threonine kinase BRAF is one of the oncoproteins that are activated by Ras. A recent study showed that microglial expression of a constitutively active form of BRAF, BRAFV600E, promoted microglia expansion and late-onset neurodegeneration in the brain.[18] Therefore we chose RasV12 to activate microglia in this work.

The aim of this study was to investigate the effects of microglial RasV12 expression in the retina. We found that RasV12 expression promoted microglial cell proliferation and migration to all regions of the retina, accompanied by aberrant MGC activation. We also found that microglial cell migration to the ONL was accompanied by photoreceptor degeneration.

Methods

All experiments adhere with the declaration of Helsinki. All animal experiments were approved by the Animal Care Committee of the Institute of Medical Science, University of Tokyo, and conducted in accordance with the ARVO (Association for Research in Vision and Ophthalmology) statement for the use of animals in ophthalmic and vision research.

Mice Strain, Genotyping and Tamoxifen Treatment

Wild type C57BL/6J mice were purchased from Japan SLS co. B6.129P2(C)-*Cx3cr1*$^{tm2.1(cre/ERT2)Jung}$/J (*Cx3cr1*^{CreER}) was purchased from Jackson laboratory. To express RasV12 and EGFP in the microglia, we crossed the *Cx3cr1*^{CreER} mice,[19] in which Cre-ER fusion protein encoding DNA was knock-in in into Cx3cr1 allele, with the *CAG-LSL-RasV12-IRES-Egfp* strain[20] or *CAG-LSL-Egfp mice*.[21] The double transgenic line *Cx3cr1*$^{CreER/+}$*; CAG-LSL-RasV12-IRES-EGFP* was denoted as Cx3cr1-RasV12 mice and *Cx3cr1*$^{CreER/+}$*; CAG-LSL-EGFP* as control. Genotyping of Cx3cr1-RasV12 mice and control mice was performed by PCR. The sequences of the primers are as follows; Cre-F 5′-tctagcgttcgaacgcactga-3′ Cre-R 5′-caccatttttttctgacccg-3′, LSL-GFP-F 5′-cagtcagttgcacaat-3′, LSL-GFP-R 5′-atatcaccagctcaccgtctt-3′, RasV12-F 5′-cactgtggaatctcggcagg-3′, RasV12-R 5′-gcaatatggtgaaaataac-3′. For both control and Cx3cr1-RasV12 mice, we did not use the mice having homozygous Cre-ER allele. For administration of tamoxifen, 50 µL of Tamoxifen dissolved in cone oil (20 mg/mL; Sigma-Aldrich, St. Louis, MO, USA) was injected subcutaneously into Cx3cr1-RasV12 mice and control mice at postnatal day 14. Mice were harvested at one, three, five, and seven days after injection.

Hematoxylin and Eosin (H&E) Staining

Brain and retina were isolated after perfusion fixation using 4% paraformaldehyde (PFA) in PBS and fixed overnight in the same solution at 4°C. The samples were embedded into paraffin and sectioned (4 µm). After deparaffinization, the sections were stained with hematoxylin solution (Fujifilm Wako Pure Chemical, Osaka, Japan) for 10 minutes and washed by water for 30 minutes and stained with Eosin (Muto Pure Chemicals, Tokyo, Japan). The sections were washed by ethanol for 20 minutes and then xylene for 15 minutes and mounted using Malinol (Muto Pure Chemicals, Tokyo, Japan).

Immunohistochemistry

Immunohistochemistry of frozen sectioned retinas was performed as previously described.[22] Brain was isolated after perfusion fixation using 4% PFA and fixed overnight at 4°C in 4% PFA. Fixed brains were subjected to sucrose replacement and sectioned by either 10 or 16 µm thickness. Primary antibodies are mouse anti-Brn3b (1:500; Santa Cruz Biotechnology, Dallas, TX, USA), -AP-2α (1:50; DSHB, Iowa City, IA, USA), –glial fibrillary acidic protein (1:400; Sigma-Aldrich), -pERK1/2 (1:500, Cell Signaling Technology, Danvers, MA, USA), -Rhodopsin (1:200; LSL, Tokyo, Japan), Ki67 (1:100; BD Biosciences, Franklin Lakes, NJ, USA), rat anti-CD68 (1:2000, BIO-RAD, Hercules, CA, USA), rabbit anti-Calbindin (1:500), Iba1 (1:1000, FUJIFILM Wako Pure Chemical, Osaka, Japan), Recoverin (1:1000; Abcam, Cambridge, UK), active Caspase3 (1:250; Promega, Madison, WI, USA), -Tmem119 (1:250; Abcam), -NeuN (1:1000; Abcam), sheep anti-Chx10 (1:500; Exalpha Biological Inc, Shirley, MA, USA), and chicken anti-GFP (1:2000; Abcam) antibodies. The primary antibodies were detected by appropriate fluorescent conjugated secondary antibodies (Alexa Fluor 488, 594, or 680; Thermo Fisher Scientific, Waltham, MA, USA). Stained sections were observed by Axio Imager M1 microscope (Carl Zeiss, Oberkochen, Germany) or Axio Imager M2 microscope (Carl Zeiss) with AxioVison ver.4.9.1.0 software (Carl Zeiss). Orthogonal images were taken by LSM710 confocal microscope (Carl Zeiss). Z-stacked images were taken at intervals of 1 µm with ZEN 2009- and ZEN 2.3 lite-software (Carl Zeiss).

Ex Vivo Confocal Time-Lapse Imaging

Isolated retinas of Cx3cr1-RasV12 mice were placed on Millicell chamber filters (Millipore, Burlington, MA, USA) and stained with 0.01 mg/mL of Hoechst33342 (Dojindo Laboratories, Kumamoto, Japan) for 10 minutes at room temperature. Then, the retinas were embedded in 1% agarose (Nippon Gene, Tokyo, Japan) in PBS at 37°C. After agarose had the property of being solid, the filters were carefully removed from embedded retinas, and then the samples underwent time-lapsed imaging. The images were taken

Downloaded from intl.iovs.org on 04/26/2024

at 1-minute intervals, 90 times, with an LSM710 confocal microscope (Carl Zeiss). Images were edited using ZEN 2009 and ZEN 2.3 lite software (Carl Zeiss).

Flow Cytometry

Isolated retains were dissociated to a single cell level as described previously.[22] Peripheral blood was collected from tail veins, and the erythrocytes were lysed using ACK lysing buffer (Thermo Fisher Scientific). Cells were stained with PE-conjugated anti-CD11b antibody (Bio Legend, San Diego, CA, USA), Alexa Fluor647-conjugated anti-CD73 antibody (BD Biosciences), or Annexin V-PE (Bio Vison, Milpitas, CA, USA). Dead cell exclusion was done by using propidium iodide (Sigma-Aldrich). Cells were analyzed by FACS Calibur (BD Biosciences). Data analysis were performed using Flow Jo software (BD Biosciences).

RT-qPCR

Total RNA was purified from mouse whole retina using Sepasol (Nacalai Tesque, Kyoto, Japan), and cDNA was synthesized using ReverTra Ace qPCR RT Master Mix (Toyobo, Tokyo, Japan). Quantitative PCR (qPCR) was performed using the THUNDERBIRD SYBR qPCR Mix (Toyobo) and the Roche Light Cycler 96 (Roche Diagnostics, Basel, Switzerland). *Actb* and *Sdha* were used as reference genes.

Statistical Analysis

Statistical analysis was performed using R software (The R Foundation for Statistical Computing, Vienna, Austria). *P* values were calculated by Wilcoxon rank sum test (Mann-Whitney U test) using R package "exactRankTests."

Results

Generation of Mice with Inducible RasV12 Expression in Microglia

The double transgenic lines *CAG-LSL-RasV12-IRES-EGFP; Cx3cr1*$^{CreER/+}$ (Cx3cr1-RasV12 mice) and *CAG-LSL-EGFP*; *Cx3cr1*$^{CreER/+}$ (control mice) were used in this study. The chemokine receptor CX3CR1 is specifically expressed in monocytes and tissue-resident macrophages, including microglia[23]; hence, *Cx3cr1 CreER* knock-in mice expressed tamoxifen-inducible Cre recombinase in microglial cells. EGFP was also expressed after tamoxifen administration in both Cx3cr1-RasV12 mice and control mice, allowing for lineage tracing.

Cx3cr1-EGFP (control) and Cx3cr1-RasV12 mice were born at the expected Mendelian ratio (Table). Tamoxifen was administered to control and Cx3cr1-RasV12 mice at postnatal day 14 (P14). Death of unknown causes was observed in Cx3cr1-RasV12 mice nine to ten days after tamoxifen injection. Because *Cx3cr1* is also expressed in circulating monocytes,[23,24] we evaluated the presence of monocytes with Cre-mediated recombination in the peripheral blood by flow cytometry (Supplementary Fig. S1A). In Cx3cr1-RasV12 mice, EGFP expression was detected in approximately 2% of CD11b-positive cells (Supplementary Fig. S1B). In the same mice, we observed that about 50% of CD11b cells in the retina were also positive for EGFP (Supplementary Fig. S1A and S1B). Therefore we could confidently conclude that EGFP-positive cells in the retina and brain were mostly microglia and that the representation of macrophages in this population is negligible.

Characterization of RasV12-Expressing Microglia in the Retina and Brain

First, we confirmed that the numbers and distribution of microglia in the Cx3cr1-EGFP retina were the same as in wild-type mouse retina. Flow cytometry analysis showed about 1% of all retinal cells from both types of mice were CD11b-positive (Supplementary Fig. S2A). In sections, the distribution of Iba1-positive cells was indistinguishable between retinas derived from wild-type and Cx3cr1-EGFP mice (Supplementary Fig. S2B). We then evaluated the presence of RasV12-expressing microglia in the retina and the brain. Retinas harvested at day seven were frozen-sectioned for histologic examination. The number of EGFP-positive cells was considerably higher in retinas from Cx3cr1-RasV12 mice compared with control retinas (Figs. 1A, 1B). Moreover, the vast majority of EGFP-expressing cells also expressed Iba1, which is a marker of microglia and macrophages (Fig. 1C). In control retinas, EGFP$^+$Iba1$^+$ cells localized mainly in the IPL, whereas these cells were distributed throughout the Cx3cr1-RasV12 mice retinas (Fig. 1D). Resting microglia are often found in the retinal IPL and OPL.[25] In control retinas, EGFP$^+$Iba1$^+$ cells were primarily found in the IPL and OPL seven days after tamoxifen administration (Fig. 1D). By contrast, RasV12-expressing Iba1-positive cells were observed in the ganglion cell layer (GCL), ONL, and SR (Fig. 1D), suggesting microglial cell migration to the inner and outer layers of the retina.

We then examined the time course of EGFP expression at days 1, 3, 5, and 7 after tamoxifen administration. EGFP was expressed from day 3 in the retinas of control and Cx3cr1-RasV12 mice (Fig. 1E, arrowheads). EGFP-positive cells also expressed the microglia-specific marker TMEM119 (Fig. 1E).[26] EGFP$^+$TMEM119$^+$ cells accounted for nearly 90% of the total EGFP-positive cell population in control and Cx3cr1-RasV12 retinas at days 3, 5, and 7 after tamox-

Table. Genotyping Results of Cx3cr1-EGFP Mice (Upper) and Cx3cr1-RasV12 Mice (Lower)

	Expected No. (%)	Observed No. (%)
Cx3c1r1-EGFP genotypes (n = 107)		
Cre/+; +/+	54 (50%)	61 (57%)
Cre/+; EGFP/+	54 (50%)	46 (43%)
Cx3c1r1-RasV12 genotypes (n = 214)		
Cre/+; +/+	107 (50%)	118 (55%)
Cre/+; RasV12/+	107 (50%)	96 (45%)

Cx3cr1$^{CreER/CreER}$ mice were crossed with *CAG-LSL-EGFP/+* mice or *CAG-LSL-RasV12-EGFP/+* mice. Cx3cr1-EGFP and Cx3cr1-RasV12 mice were born with predicted Mendelian ratio approximately.

Investigative Ophthalmology & Visual Science

Downloaded from intl.iovs.org on 04/26/2024

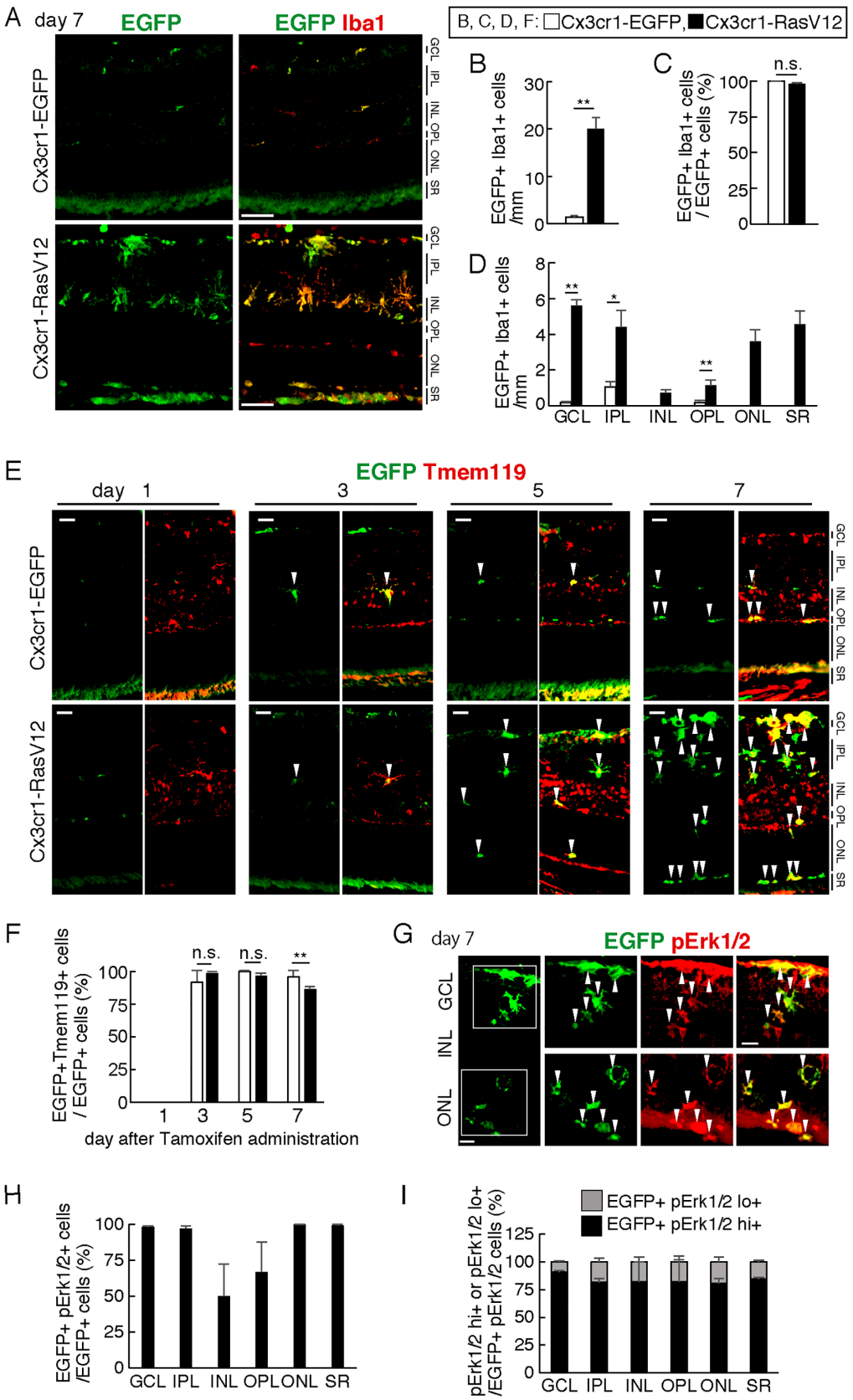

Figure 1. Expression of RasV12-EGFP in the microglia in Cx3cr1-RasV12 mouse. Cx3cr1-RasV12 or control (Cx3cr1-EGFP) mice at P14 were administered with tamoxifen, and after day 1, 3, 5, or 7, the retinas were harvested. Isolated retinas were frozen sectioned, and stained with anti-EGFP and indicated antibodies. **(A)** EGFP and Iba1 double staining patterns of day 7 retinas. *Scale bars:* 50 µm. **(B)** The number of EGFP and Iba1 double positive cells at day 7. **(C)** The population of EGFP and Iba1 double positive cells in total EGFP positive cells. **(D)**

Investigative Ophthalmology & Visual Science

Downloaded from intl.iovs.org on 04/26/2024

Distribution of EGFP and Iba1 double positive cells was measured in each retinal layer. **(E)** EGFP and Tmem119 double staining patterns in day 1, 3, 5, and 7 after tamoxifen administration. *Scale bars:* 20 µm. **(F)** The populations of EGFP and Tmem119 doble positive cells in total EGFP positive cells are shown. **(G)** EGFP and phosphorylated Erk1/2 (pErk1/2) staining patterns at day 7. *Scale bars:* 20 µm. (**H**) The population of EGFP and pErk1/2 double positive cells in the total EGFP positive cells was calculated in each region of the retina. (**I**) EGFP and pErk1/2 double positive cells were segregated to those with high or low levels of pErk1/2 signals, and population was calculated. Graphs show mean of six samples from independent mice with SEM. *P* values were calculated by Mann-Whitney U test. * $P < 0.05$, ** $P < 0.01$, n.s., not significant.

ifen administration (Fig. 1F). Furthermore, immunohistochemical analysis revealed the presence of phosphorylated ERK1/2 (pErk1/2) in EGFP-positive microglia in Cx3cr1-RasV12 retinas (Fig. 1G, arrowheads), confirming Ras signaling pathway activation in these microglial cells. The population of EGFP and pErk1/2 double positive cells in the Cx3cr1-RasV12 retina was slightly smaller in the INL and OPL compared with other regions, but the differences were not statistically significant (Fig. 1H). There were strong and weak pErk1/2 signals in EGFP-positive cells, but the populations were similar in all regions (Fig. 1I). In the brains of Cx3cr1-RasV12 mice, we observed prominent EGFP expression in the ventral orbital cortex (VO), lateral orbital cortex (LO), and ventral tenia tecta (VTT) at day 7 after tamoxifen administration (Supplementary Fig. S3A). Hematoxylin and eosin staining confirmed strong nuclear staining in these regions of the brain (Supplementary Fig. S3B). We then examined expression of pan-neuron marker NeuN by immunostaining of frozen sections. We observed similar NeuN expression pattern and number of NeuN positive cells in brains of control and Cx3cr1-RasV12 mice (Figs. S3C, S3D), suggesting that the brain neuron degeneration may not occurred in this situation. Similar to what we observed in the retina, EGFP expression was apparent from day 3 in the orbital cortex region of the brain (Supplementary Fig. S4A), and EGFP-positive cells also expressed Iba1 (Supplementary Fig. S4A, arrowheads, Supplementary Fig. S4B). The number of $EGFP^+Iba1^+$ cells continuously increased in the brain of Cx3cr1-RasV12 mice (Supplementary Fig. S4C). Moreover, ERK1/2 phosphorylation was detected in EGFP-positive cells in the brain of Cx3cr1-RasV12 mice (Supplementary Fig. S4D, arrowheads).

Migration and Proliferation of RasV12-Expressing Microglia

We then examined more details of transition of microglia after tamoxifen administration in the Cx3cr1-RasV12 retina. The number of $EGFP^+TMEM119^+$ cells constantly increased in Cx3cr1-RasV12 retinas, whereas only a slight increase was observed in control retinas (Figs. 2A, B). At day 7 after tamoxifen administration, retinas from Cx3cr1-RasV12 mice contained a significantly higher number of $EGFP^+TMEM119^+$ cells compared with control retinas (Figs. 2A, 2B). Additionally, retinas from Cx3cr1-RasV12 mice contained a significantly higher number of proliferating microglial cells ($Ki67^+EGFP^+$; Fig. 2C, arrowheads). $Ki67^+EGFP^+$ cells comprised nearly 70% of the total EGFP-positive cell population in retinas from Cx3cr1-RasV12 mice (Fig. 2D). Although $Ki67^+EGFP^+$ cells were present in all retinal layers, notably high numbers were observed in the inner and outer layers (Fig. 2E).

RasV12-expressing microglia exhibited ameboid morphology with a large cell body and short pseudopodia (Fig. 2C), which is typically observed in activated microglia.[27,28] Consistently, *Ccl2*, *Ccl3*, *Cxcl1*, *Cxcl5*, *Il1b, Il6*, and *Tnf* were significantly upregulated in Cx3cr1-RasV12 retinas (Fig. 2F), further supporting microglial activation.[29,30] In the brain, although a significant number of EGFP-positive cells expressed Ki67 (Supplementary Figs. S5A, S5B), Ki67-positive cells comprised less than 30% of the total EGFP-positive cell population (Supplementary Fig. S5C).

RasV12 Expression in Microglia Promotes Photoreceptor Degeneration

Histological analysis indicated the loss of photoreceptors in Cx3cr1-RasV12 retinas (Fig. 3A, arrowheads). Immunohistochemical staining revealed that microglial cells were localized close to the degenerating regions of the ONL (Fig. 3B). Moreover, differential interference contrast (DIC) imaging showed a reduction in the thickness of the outer segments of Cx3cr1-RasV12 retinas (Figs. 3B, C). We also performed Annexin V staining to measure apoptosis[31] and found an increased number of apoptotic cells in Cx3cr1-RasV12 retinas. Importantly, the number of apoptotic cells was higher in CD73-positive rod photoreceptor cells than other retinal cells (Figs. 3D, E). In Cx3cr1-RasV12 retinas, we also observed upregulation of *Edn2* and *Fgf2* (Fig. 3F), which are commonly induced upon photoreceptor damage.[8]

Retinal degeneration is often accompanied by reactive gliosis, which is characterized by strong glial fibrillary acidic protein (GFAP) expression.[32] Consistently, GFAP was upregulated in Cx3cr1-RasV12 retinas (Figs. 3G, 3H), and microglia were localized adjacent to the GFAP-positive MGCs (Fig. 3G, enlarged panels). We found no differences in the numbers of RBPMS-positive retinal ganglion cells (Supplementary Fig. S6A), AP-2α-positive amacrine cells (Supplementary Fig. S6B), Chx10-positive bipolar cells (Supplementary Fig. S6C), and Calbindin-positive horizontal cells (Supplementary Fig. S6D) in RasV12-expressing and control retinas, suggesting that survival and maintenance of these cell types was not affected by RasV12 expression in microglia.

RasV12-Expressing Microglia in the ONL, but not in the INL, Mediates Rod Photoreceptor Phagocytosis

Confocal microscopy revealed that RasV12-expressing microglia engulfed recoverin-positive rod photoreceptors in the damaged ONL regions (Fig. 4A); hence, we measured phagocytosis related molecules in Cx3cr1-RasV12 retinas. In Cx3cr1-RasV12 mice, EGFP-positive cells strongly expressed CD68 (Fig. 4B, arrowheads), which is a lysosomal protein highly expressed in activated microglia.[7,33] Interestingly, the number of CD68-expressing cells was higher in the ONL and SR than in the inner layers of the retina (Fig. 4C). Furthermore, population of the $EGFP^+CD68^+TMEM119^+$ cells in

Investigative Ophthalmology & Visual Science

Downloaded from intl.iovs.org on 04/26/2024

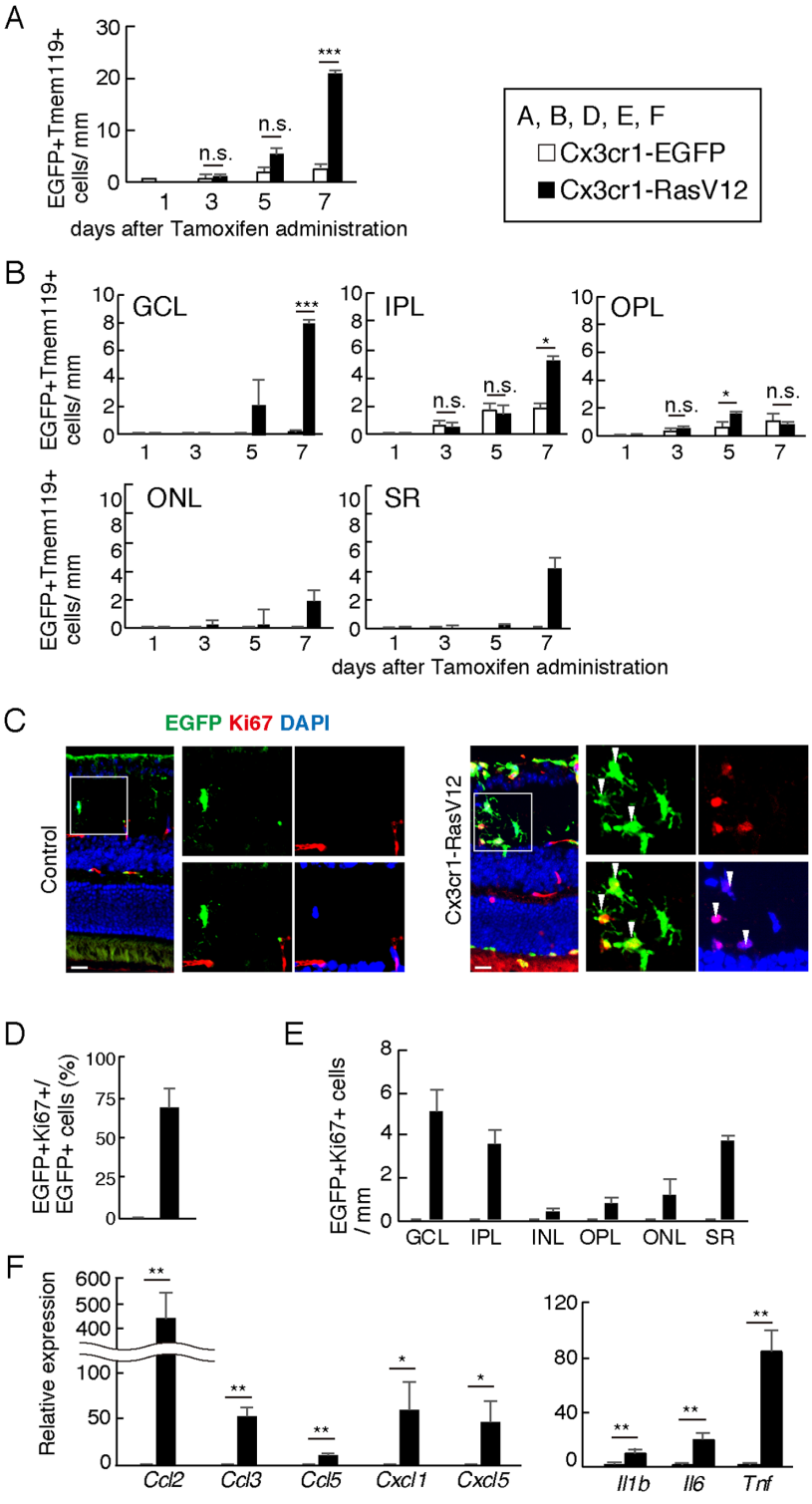

Figure 2. RasV12 expressing microglia accumulated in both inner and outer layers of the retina. **(A)** Number of EGFP and Tmem119 double positive cells after tamoxifen administration in retinas of control (Cx3cr1-EGFP) and Cx3cr1-RasV12 mice. Immunohistochemistry panels are shown as Figure 1E. (**B**) Distribution of RasV12/EGFP or control EGFP expressing-microglia in the retina. Quantification of number of EGFP and Tmem119 double positive cells in GCL, IPL, ONL, and SR are shown. (**C–E**) Proliferation of the microglia was examined by the immunohistochemical analysis of Ki67. **(C)** Immunostaining patterns of anti-EGFP and -Ki67 antibodies of day 7 retinas. Nuclei were visualized with staining by DAPI. *Scale bars:* 20 µm. **(D)** The population of EGFP and Ki67 double positive cells in total EGFP positive cells. **(E)** Distribution of EGFP and Ki67 double positive cells. **(F)** Expression of transcripts of various chemokines and cytokines was examined by RT-qPCR retinas of Cx3cr1-RasV12 or control mice at day 7 after tamoxifen administration. In **(B)** and **(F)**, the data of graphs are mean with SEM from six samples of independent mice. *P* values were calculated by Mann-Whitney U test. * $P < 0.05$, ** $P < 0.01$, *** $P < 0.001$, n.s., not significant. In **(D)** and **(E)**, graphs show mean with SEM from three samples of independent mice.

Investigative Ophthalmology & Visual Science

Downloaded from intl.iovs.org on 04/26/2024

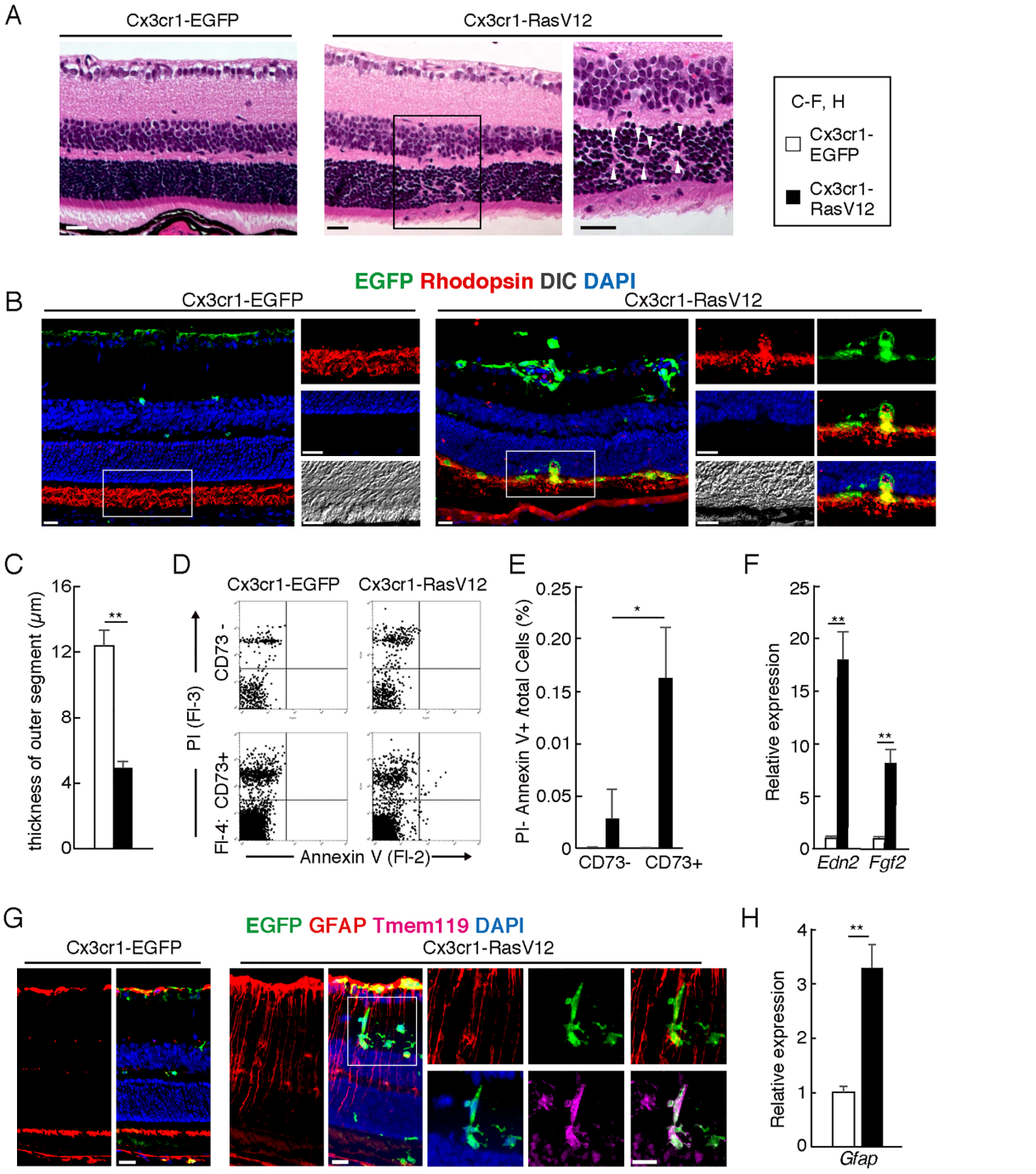

Figure 3. Perturbed ONL structure and activated Müller glia in Cx3cr1-RasV12 retina. **(A)** Paraffin sectioned retinas of control (Cx3cr1-EGFP) or Cx3cr1-RasV12 mice were subjected to H&E staining. *Right panel* of Cx3cr1-RasV12 section is enlarged view of black squared region in the *middle panel*. *White arrowheads* indicate spotted missing of photoreceptors. *Scale bars*: 20 μm. **(B)** Frozen sectioned retinas of control or Cx3cr1-RasV12 were subjected to immunohistochemistry using anti-EGFP, -Rhodopsin antibody, and nuclei were visualized by staining with DAPI. DIC images are shown. *Scale bars*: 20 μm. **(C)** Thickness of outer-segment was measured from DIC pictures in control and Cx3cr1 mice retina. **(D, E)** Flow cytometrical analysis of retinal cells of control and Cx3cr1-RasV12 retinas by staining with Annexin V, CD73, and PI. Dot blot patterns of Annexin V and propidium iodide (PI) of CD73 negative (*upper panels*) and CD73 positive (*lower panels*) are shown. PI negative/Annexin V positive cell population in CD73 negative or positive population of Cx3cr1-RasV12 retina are shown. **(F)** Expression levels of *Edn2* and *Fgf2* transcripts by RT-qPCR in control and Cx3cr1-RasV12 retinas at day 7. **(G)** Frozen sections of control or Cx3cr1-RasV12 mice derived retinas were stained with anti-EGFP, -GFAP, and -Tmem119 antibodies. Nuclei were visualized with DAPI staining. **(H)** The expression level of *Gfap* transcripts of control or Cx3cr1-RasV12 retina was examined by RT-qPCR. In **(C), (F),** and **(H),** the graphs are mean of six independent samples with SEM. In **(E)**, values in the graph are mean with SEM from four samples of independent mice. *P* values were calculated by Mann-Whitney U test. $^{*}P < 0.05$, $^{**}P < 0.01$.

Investigative Ophthalmology & Visual Science

Downloaded from intl.iovs.org on 04/26/2024

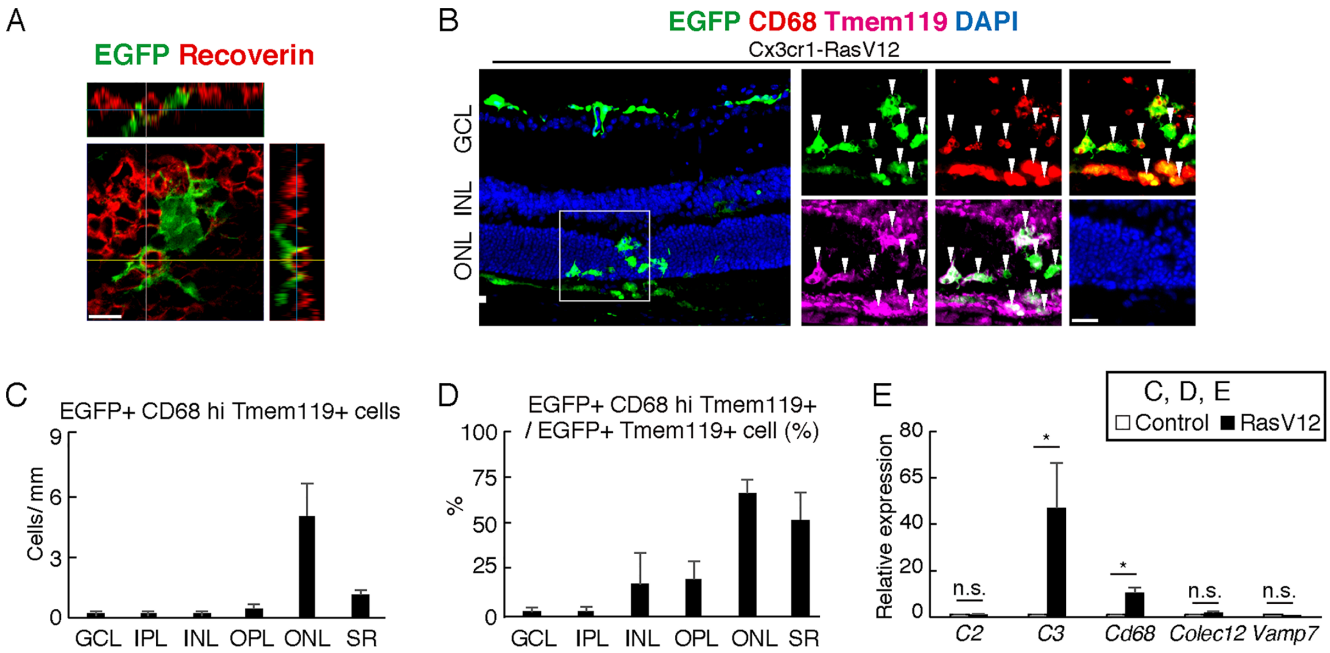

Figure 4. The expression of phagocytosis related molecules in Cx3cr1-RasV12 mice retina. **(A)** Orthological view of EGFP and Recoverin antibodies stained retina of Cx3cr1-RasV12 mice at day 7. *Scale bar*: 10 µm. **(B–D)** Frozen sections of retinas of control (Cx3cr1-EGFP) and Cx3cr1-RasV12 mice at day 7 after tamoxifen administration were subjected to immunohistochemistry using anti-EGFP, -CD68, and -Tmem119 antibodies. Nuclei were visualized with DAPI in some panels. *White arrowheads* indicate EGFP, CD68 and Tmem119 triple positive cells in ONL in (**B**). *Scale bars*: 20 µm. In (**C**), number of EGFP, CD68, and Tmem119 triple positive cells in subregions of the retina was counted, and cell number in each sub-region in 1mm width of the section. In (**D**), the population of the triple positive cells in EGFP and Tmem119 double positive cells (%) in subregions of the retina. **(E)** Expression of transcripts of various phagocytosis related genes in control (Cx3cr1-EGFP) and Cx3cr1-RasV12 retina were examined by RT-qPCR. In **(C), (D)**, and **(E),** graphs show mean of counting from six independent samples with SEM. *P* values were calculated by Mann-Whitney U test. $^*P < 0.05$, n.s., not significant.

EGFP and Tmem119 double positive cells was considerably higher in the ONL and SR than in other retinal regions (Fig. 4D). Phagocytosis-related genes *C3* and *Cd68* were upregulated in Cx3cr1-RasV12 retinas (Fig. 4E).

The Behavior of RasV12-Expressing Microglia Differs in the IPL and ONL

We next examined the behavior of RasV12-expressing microglia in different regions of the retina. We prepared retinal explants from Cx3cr1-RasV12 mice and labeled the nuclei of rod photoreceptors with Hoechst33342. Time-lapse imaging revealed that RasV12-expressing microglia in the ONL engulfed photoreceptors by extending their pseudopodia. Moreover, multiple nuclei were observed in individual microglial cells, suggesting rod photoreceptor engulfment by microglia (Fig. 5, upper panel, Supporting information movie 1). However, we found no evidence of cells engulfment by RasV12-expressing microglia in the IPL (Fig. 5, lower panel, Supporting information movie 2).

Discussion

In this study, we examined the role of microglia in retina by inducing the expression of constitutively active Ras (RasV12) in microglial cells. RasV12 expression promoted microglial activation, which led to the degeneration of retinal photoreceptors.

Most studies on the molecular mechanisms of microglia used photoreceptor degeneration models, suggesting that the initial event of inflammatory cascade is photoreceptor injury. *Edn2* upregulation has been reported in injured photoreceptors, and EDN2 contributes to the activation of MGCs.[9] Similarly, transcription of *Lif* is induced upon tissue damage, and its expression induces activation of MGCs, which is characterized by GFAP expression. Photoreceptor degeneration initiated by an inflammatory network has been well documented, and the roles of microglia have been characterized in such models, especially by suppressing microglial activity through drug administration.[6,7,34,35] However, we believe that these models have limited utility for examining the primary effects of activated microglia in healthy retinas. In this study, we found evidence of *Edn2* and *Lif* transcriptional activation in Cx3cr1-RasV12 retinas. Therefore, RasV12 expression in microglia is sufficient to induce *Edn2* expression in the absence of injury of photoreceptors, and in photoreceptor degeneration mouse models, *Edn2* upregulation is likely induced at least partly by microglia. Alarmin is expressed at the initial phase of photoreceptor degeneration, and it may contribute to microglial activation during early degeneration. On the other hand, EDN2 is known to exert protective effects on photoreceptors. Therefore microglia may modulate retinal degeneration through upregulation of EDN2 on rod photoreceptors in certain situation.

Another model showed that aberrant activation of microglia causes retinal degeneration is based on attenuation of TGF-β signaling.[36] Ablation of the TGF-β receptors in the microglia of adult mice resulted in abnormal microglial numbers and activation. Furthermore, secondary gliotic changes and neuronal apoptosis were observed.

Downloaded from intl.iovs.org on 04/26/2024

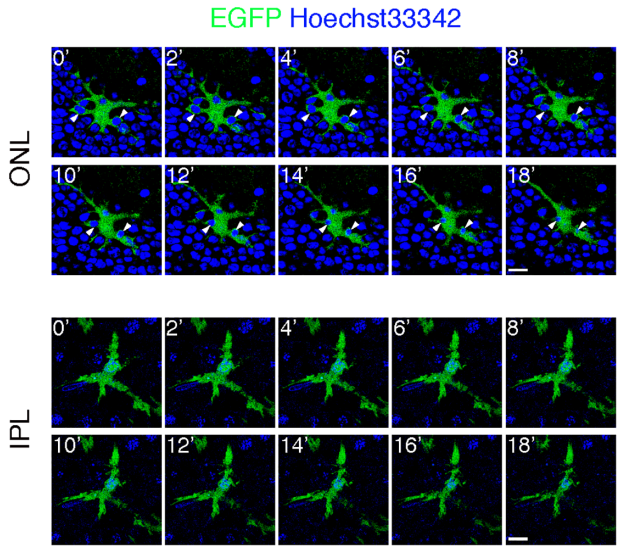

Figure 5. Phagocytosis of photoreceptors by RasV12-expressing microglia were observed in ONL but not observed in IPL. Time-lapse analysis in Cx3cr1-RasV12 retinal explant. EGFP positive cell phagocytosed nuclear in ONL (*upper panels*), but did not show phagocytotic feature in IPL (*lower panels*). *White arrowheads* indicate phagocytosed nuclei by EGFP positive cell. Panels show pictures in two-minute intervals. *Scale bars*: 10 µm. Movies are up-loaded as supporting information.

CX3CL1-CX3CR1 signaling is known to negatively regulate microglia, as shown in gain- and loss-of-function analyses. Constitutive CX3CR1 signaling repressed microglial activation, and in the uninjured adult retina, the ablation of CX3CL1-CXCR1 signaling does not lead to gross changes in retinal morphology[37]; however, CX3CR1-deficient microglia in the rd10 retina was associated with accelerated photoreceptor degeneration.[7,38] These reports, together with our current results, support the idea that aberrant microglia activation causes neuronal damage, in accordance with the studies suggesting roles of microglia in age-related retinal degenerative pathology. BRAFV600E mutation has been implicated in late-onset neurodegenerative diseases and histiocytosis.[39,40] Mosaic expression of BRAFV600E in the yolk-sac erythro-myeloid progenitors resulted in clonal expansion of microglia and late-onset neurodegeneration in the brain.[18] Our RasV12 microglial activation model shared some features with this BRAFV600E-expressing model, including the expansion of Iba1-positive cells, GFAP expression, and inflammatory cytokine expression. However, our RasV12-expressing microglia mouse model exhibited early-onset microglial activation in the brain and neural degeneration in the retina. Furthermore, our mice did not survive more than nine days after tamoxifen administration. On the other hand, no description about early phenotype of BRAFV600E expressing model was available; therefore we could not directly compare the findings acquired from these two animal models. Considering that Ras acts upstream of BRAF and activates not only the MAPK pathway but also multiple other signaling pathways, it is not surprising that our RasV12-expressing microglia model has a more complex phenotype than the BRAFV600E-expressing model.

Interestingly, Ras activation in microglia resulted in cell migration towards the inner and outer layers of the retina. Because ERK1/2 activates various migration-related molecules, such as MLCK, Paxillin, FAK, and Calpain,[41] the enhanced migration of RasV12-expressing microglia was anticipated; however, we could not explain the tropism observed in microglia migration patterns. In photoreceptor degeneration models, microglia migrated primarily into degeneration sites; however, the molecules promoting cell migration could not be identified. In this study, we found that RasV12-expressing microglia were localized close to MGCs; thus it is likely that microglial cells migrated along the migration pathway of MGCs. However, no determinant of inner or outer direction is hypothesized currently, and diffused migration is rather plausible.

We observed enhanced expression of inflammatory cytokines in RasV12-expressing microglia. These inflammatory stimuli may have contributed to rod photoreceptor apoptosis and subsequent phagocytosis by RasV12-expressing microglia. Interestingly, we could not detect degeneration of non-photoreceptor cells or phosphatidylserine (PS) expression on CD73-negative cells in Cx3cr1-RasV12 retinas. Moreover, the cellular dynamics of RasV12-expressing microglia were profoundly different in the ONL and IPL. These results suggest that constitutive microglial activation induced retinal degeneration, and microenvironment cues may modulate the microglial phenotypic features and effects of microglial activation. Future studies are required to examine the role of the immunosuppressive microenvironment of the inner side of the retina.

Acknowledgments

The authors thank Miho Nagoya for excellent technical assistance and Yukihiro Baba for fruitful discussion.

Disclosure: **Y. Moriuchi,** None; **T. Iwagawa,** None; **A. Tsuhako,** None; **H. Koso,** None; **Y. Fujita,** None; **S. Watanabe,** None

References

1. Kierdorf K, Prinz M. Microglia in steady state. *J Clin Invest*. 2017;127(9):3201–3209, doi:10.1172/JCI90602.
2. Salter MW, Stevens B. Microglia emerge as central players in brain disease. *Nat Med*. 2017;23(9):1018–1027.
3. Silverman SM, Wong WT. Microglia in the retina: roles in development, maturity, and disease. *Annu Rev Vis Sci*. 2018;4(1):45–77.
4. Santos AM, Martín-Oliva D, Ferrer-Martín RM, et al. Microglial response to light-induced photoreceptor degeneration in the mouse retina. *J Comp Neurol*. 2010;518(4):477–492.
5. Ng TF, Streilein JW. Light-induced migration of retinal microglia into the subretinal space. *Investig Ophthalmol Vis Sci*. 2001;42(13):3301–3310.
6. Zhao L, Zabel MK, Wang X, et al. Microglial phagocytosis of living photoreceptors contributes to inherited retinal degeneration. *EMBO Mol Med*. 2015;7(9):1179–1197.
7. Tipoe GL, Wang K, Lin B, Xiao J, So K-F, Peng B. Suppression of microglial activation is neuroprotective in a mouse model of human retinitis pigmentosa. *J Neurosci*. 2014;34(24):8139–8150.
8. Rattner A. The genomic response to retinal disease and injury: evidence for endothelin signaling from photoreceptors to glia. *J Neurosci*. 2005;25(18):4540–4549.
9. Joly S, Lange C, Thiersch M, Samardzija M, Grimm C. Leukemia inhibitory factor extends the lifespan of injured photoreceptors in vivo. *J Neurosci*. 2008;28(51):13765–13774.

Downloaded from intl.iovs.org on 04/26/2024

10. Ueki Y, Wang J, Chollangi S, Ash JD. STAT3 activation in photoreceptors by leukemia inhibitory factor is associated with protection from light damage. *J Neurochem*. 2008;105(3):784–796.
11. Holtkamp GM, Kijlstra A, Peek R, De Vos AF. Retinal pigment epithelium-immune system interactions: cytokine production and cytokine-induced changes. *Prog Retin Eye Res*. 2001;20(1):29–48.
12. Simanshu DK, Nissley D V., McCormick F. RAS proteins and their regulators in human disease. *Cell*. 2017;170(1):17–33.
13. Pixley FJ, Stanley ER. CSF-1 regulation of the wandering macrophage: complexity in action. *Trends Cell Biol*. 2004;14(11):628–638.
14. Song X, Tanaka S, Cox D, Lee SC. Fcγ receptor signaling in primary human microglia: differential roles of PI-3K and Ras/ERK MAPK pathways in phagocytosis and chemokine induction. *J Leukoc Biol*. 2004;75(6):1147–1155.
15. Colonna M, Wang Y. TREM2 variants: new keys to decipher Alzheimer disease pathogenesis. *Nat Rev Neurosci*. 2016;17(4):201–207.
16. Prior IA, Hood FE, Hartley JL. The frequency of Ras mutations in cancer. *Cancer Res*. 2020;80(14):2969–2974.
17. Brahmachari S, Jana A, Pahan K. Sodium benzoate, a metabolite of cinnamon and a food additive, reduces microglial and astroglial inflammatory responses. *J Immunol*. 2009;183(9):5917–5927.
18. Mass E, Jacome-Galarza CE, Blank T, et al. A somatic mutation in erythro-myeloid progenitors causes neurodegenerative disease. *Nature*. 2017;549(7672):389–393.
19. Yona S, Kim KW, Wolf Y, et al. Fate mapping reveals origins and dynamics of monocytes and tissue macrophages under homeostasis. *Immunity*. 2013;38(1):79–91.
20. Kon S, Ishibashi K, Katoh H, et al. Cell competition with normal epithelial cells promotes apical extrusion of transformed cells through metabolic changes. *Nat Cell Biol*. 2017;19(5):530–541.
21. Kawamoto S, Niwa H, Tashiro F, et al. A novel reporter mouse strain that expresses enhanced green fluorescent protein upon Cre-mediated recombination. *FEBS Lett*. 2000;470(3):263–268.
22. Koso H, Tsuhako A, Lai CY, et al. Conditional rod photoreceptor ablation reveals Sall1 as a microglial marker and regulator of microglial morphology in the retina. *Glia*. 2016;64(11):2005–2024.
23. Wolf Y, Yona S, Kim K-W, Jung S. Microglia, seen from the CX3CR1 angle. *Front Cell Neurosci*. 2013;7(March):1–9, doi:10.3389/fncel.2013.00026.
24. Landsman L, Liat BO, Zernecke A, et al. CX3CR1 is required for monocyte homeostasis and atherogenesis by promoting cell survival. *Blood*. 2009;113(4):963–972.
25. Rashid K, Akhtar-Schaefer I, Langmann T. Microglia in retinal degeneration. *Front Immunol*. 2019;10(AUG):1–19.
26. Bennett ML, Bennett FC, Liddelow SA, et al. New tools for studying microglia in the mouse and human CNS. *Proc Natl Acad Sci*. 2016;113(12):E1738–E1746.
27. Rathnasamy G, Foulds WS, Ling EA, Kaur C. Retinal microglia – A key player in healthy and diseased retina. *Prog Neurobiol*. 2018;(March):1–23.
28. Ulland TK, Song WM, Huang SCC, et al. TREM2 maintains microglial metabolic fitness in Alzheimer's disease. *Cell*. 2017;170(4):649–663.e13.
29. Nakagawa Y, Chiba K. Role of microglial M1/M2 polarization in relapse and remission of psychiatric disorders and diseases. *Pharmaceuticals*. 2014;7(12):1028–1048.
30. Franco R, Fernández-Suárez D. Alternatively activated microglia and macrophages in the central nervous system. *Prog Neurobiol*. 2015;131:65–86.
31. Vermes I, Haanen C, Steffens-Nakken H, Reutellingsperger C. A novel assay for apoptosisFlow cytometric detection of phosphatidylserine expression on early apoptotic cells using fluorescein labelled Annexin V. *J Immunol Methods*. 1995;184(1):39–51
32. Ekstrom P, Sanyal S, Narfstrom K, Chader GJ, Van Veen T. Accumulation of glial fibrillary acidic protein in Muller radial glia during retinal degeneration. *Investig Ophthalmol Vis Sci*. 1988;29(9):1363–1371.
33. Amadio S, Parisi C, Montilli C, Carrubba AS, Apolloni S, Volonté C. P2Y(12) receptor on the verge of a neuroinflammatory breakdown. *Mediators Inflamm*. 2014;2014:975849.
34. Arroba AI, Álvarez-Lindo N, van Rooijen N, de la Rosa EJ. Microglia-mediated IGF-I neuroprotection in the rd10 mouse model of retinitis pigmentosa. *Investig Ophthalmol Vis Sci*. 2011;52(12):9124–9130.
35. Lew DS, Mazzoni F, Finnemann SC. Microglia Inhibition Delays Retinal Degeneration Due to MerTK Phagocytosis Receptor Deficiency. *Front Immunol*. 2020;11(July):1–15.
36. Ma W, Silverman SM, Zhao L, et al. Absence of TGFβ signaling in retinal microglia induces retinal degeneration and exacerbates choroidal neovascularization. *Elife*. 2019;8:1–28.
37. Luhmann UFO, Lange CA, Robbie S, et al. Differential modulation of retinal degeneration by Ccl2 and Cx3cr1 chemokine signalling. *PLoS One*. 2012;7(4):e35551.
38. Zabel MK, Zhao L, Zhang Y, et al. Microglial phagocytosis and activation underlying photoreceptor degeneration is regulated by CX3CL1-CX3CR1 signaling in a mouse model of retinitis pigmentosa. *Glia*. 2016;64(9):1479–1491.
39. Haroche J, Charlotte F, Arnaud L, et al. High prevalence of BRAF V600E mutations in Erdheim-Chester disease but not in other non-Langerhans cell histiocytoses. *Blood*. 2012;120(13):2700–2703.
40. Berres ML, Lim KPH, Peters T, et al. BRAF-V600E expression in precursor versus differentiated dendritic cells defines clinically distinct LCH risk groups. *J Exp Med*. 2014;211(4):669–683.
41. Huang C. MAP kinases and cell migration. *J Cell Sci*. 2004;117(20):4619–4628.

Investigative Ophthalmology & Visual Science

Downloaded from intl.iovs.org on 04/26/2024